Electronic Supplementary Material (ESI) for Materials Chemistry Frontiers.

A synergistic strategy for fabricating ultralight and thermal insulating aramid nanofibers/polyimide aerogel

Xinhai Zhang[1], Xingxing Ni[1], Meiyun He[1], Yujie Gao[1], Chenxi Li[1], Xiaoliang Mo[1], Gang Sun[2], Bo You[1]*

1. Department of Materials Science, Advanced Coatings Research Center of Ministry of Education of China, Fudan University, Shanghai 200433, People's Republic of China.
2. Department of Aeronautics and Astronautics, Fudan University, Shanghai 200433, People's Republic of China.

□ Corresponding author: Bo You

Corresponding Author E-mail: youbo@fudan.edu.cn

Unlike electrostatic spinning to prepare nanofibers, ANF was produced from "Kevlar fibers" (poly-p-phenylene terephthamide, PPTA, aramid) by a chemical splitting method on a large scale and can even be obtained from discarded aramid products. Macroscale Kevlar fibers (Figure S1a) were split into nanofiber (ANF) in a DMSO/KOH/H_2O system that H_2O acted as a role for proton donor-assisted deprotonation. The split macroscale fibers dispersion showed homogeneous and brownish red. The as-prepared dispersion leaded to an evident Tyndall effect, demonstrating that the Kevlar fibers were not dissolved simply, as the inset shown in Figure S1b. The ANF precipitated when deionized water was added into the dispersion and then the precipitated ANF was washed (Figure S1b). The split mechanism is explained that hydrogen bonds of molecule chains of PPTA reduced and the electrostatic repulsions increased (Figure S1d). [1] The TEM image showed nanofiber scale of the ANF around 50 nm diameters matching those of nanowires and nanotubes, [2] as shown in Figure S1c.

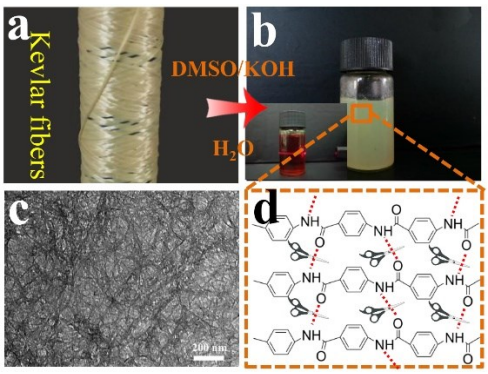

Figure S1. (a) Kevlar macro fibers. (b) ANF dispersion digital image (inset, an evident Tyndall effect of ANF dispersion). (c) TEM images of the ANF, (d) the hydrogen bonds to be weakened among molecule chains.

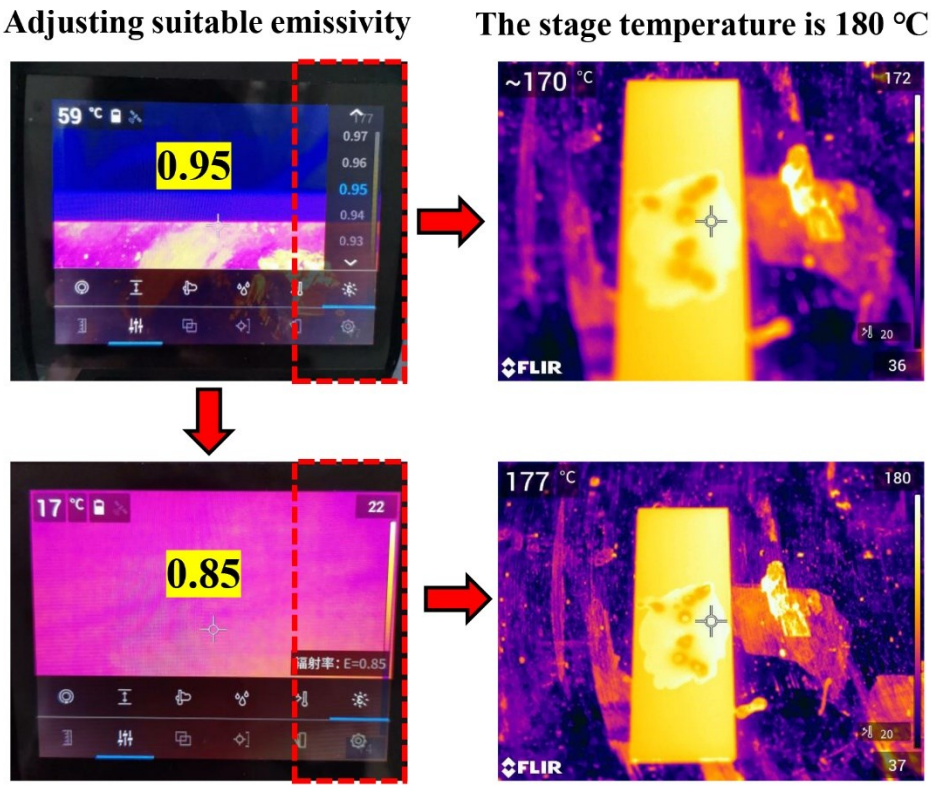

Figure S2. The adjusting process about the emissivity of the FLIR-E75. The raw materials of the ANF/PI aerogel was heating to 180 ℃， and then we constantly adjust the radiation coefficient until the FTIR-E75 can show the closest temperature to 180 ℃. This value (0.85) is the approximate value of the emissivity of the material.

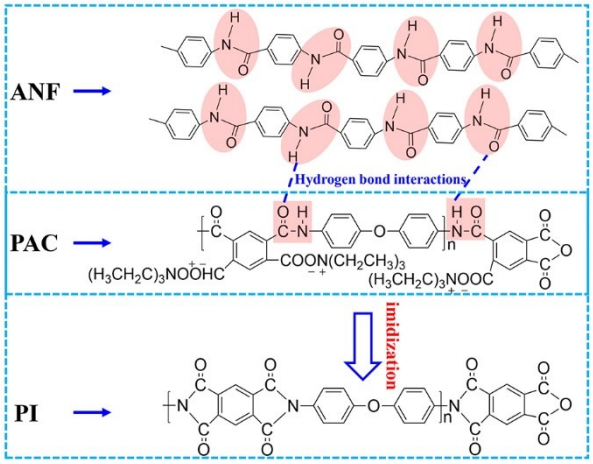

Figure S3. The chemical structures of the ANF, PAC and PI, hydrogen bond interaction between ANF and PAC, and the imidization process.

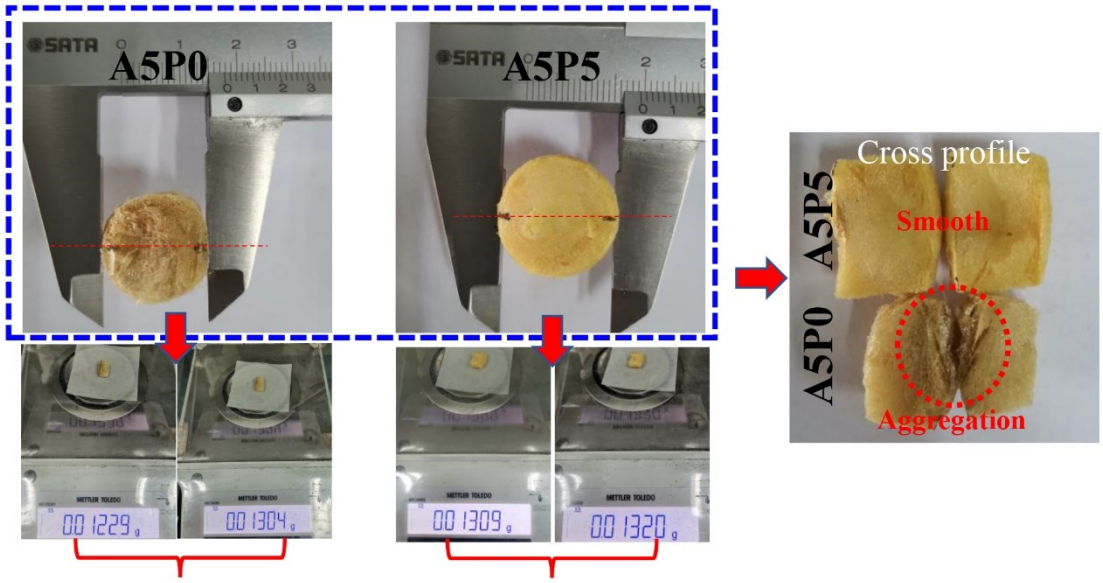

Figure S4. The uniformity of the A5P0 aerogel and A5P5 aerogel. We cut the A5P0 aerogel and A5P5 aerogel in halves down the middle, weighing them respectively, as shown in Figure S4. According to the images of cross profile of the two aerogels, the A5P0 aerogel was more rough cross profile than that of A5P5 aerogel because of the severe aggregation of pure ANF. Furthermore, the weight ratio of two pieces of the aerogel was calculated. Generally, the closer that this ratio value is to 1, the more uniform the aerogel is. Obviously, the value of the weight ratio of the A5P5 aerogel is closer to 1.

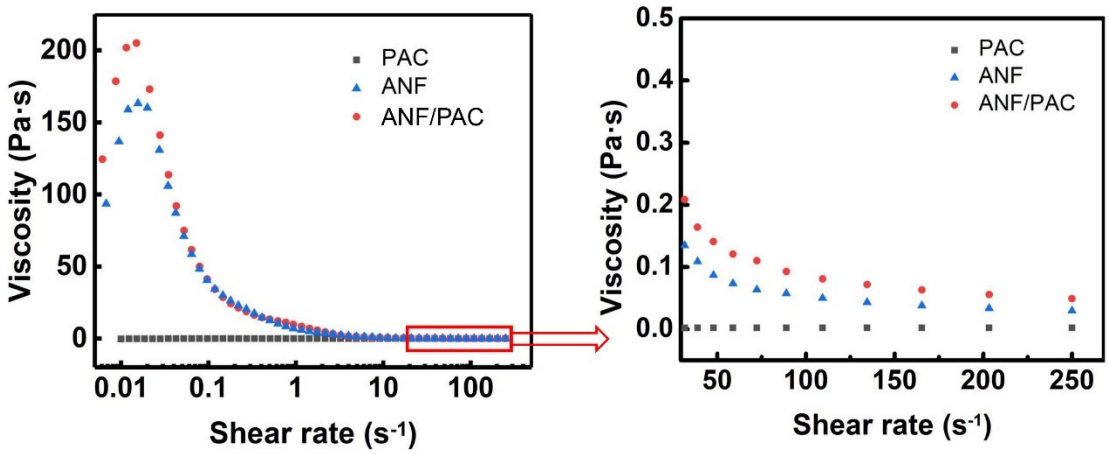

Figure S5. The shear curves of PAC solution, ANF dispersion, and ANF/PAC mixture.

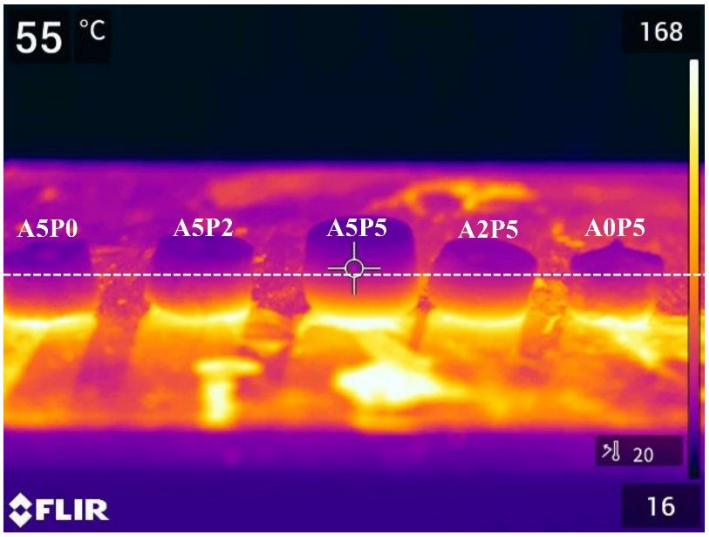

Figure S6. The thermal insulation of these aerogel with same thickness (white dotted line) recorded by an infrared camera.

Supplementary Note 1. The thermal conductivity of the aerogel.

The total thermal conductivity of aerogel is calculated as following eq. (1): [3]

$$\lambda_{total} = \lambda_s + \lambda_g + \lambda_c + \lambda_r \quad (1)$$

where λs is the solid thermal conductivity, λg is the gas thermal conductivity, λc is the convective heat transfer coefficient, and λr is the radiative heat transfer coefficient.

The thermal conductivity of the gas (λ_g) is considered to be the main contributor to the total thermal conductivity of aerogels and obeys the following eq. (2). [4] According to equation (2), a smaller pore size is associated with a lower thermal conductivity.

$$\lambda_g = \frac{\lambda_g^0}{1 + \alpha l_{mfp} / l_{cl}} \quad (2)$$

where $\lambda_g{}^0$ is the thermal conductivity of the free air, α is a constant with a value of approximately 2 for air, l_{mfp} is the mean free path of a gas molecule (70 nm), and l_{cl} is the average pore diameter.

The solid thermal conductivity (λ_s) is the product of the thermal conductivity of the compact solid material and the volume fraction, demonstrating that the low density is very important for the low thermal conductivity. The low density will lead to high porosity (P), according to the eq. (3): [5]

$$P = (1 - \frac{\rho_v}{\rho^*}) \times 100\% \quad (3)$$

where ρ_v is the bulk density, ρ^* is the true density of the material.

Thus, both low density and high porosity are helpful for realizing the excellent thermal insulation.

References

1. B. Yang, L. Wang, M. Zhang, J. Luo and X. Ding, Timesaving, High-Efficiency Approaches to Fabricate Aramid Nanofibers, *ACS Nano*, 2019, **13**, 7886-7897.

2. M. Yang, K. Cao, L. Sui, Y. Qi, J. Zhu, A. Waas, E. M. Arruda, J. Kieffer, M. D. Thouless and N. A. Kotov, Dispersions of Aramid Nanofibers: A New Nanoscale Building Block, *ACS Nano*, 2011, **5**, 6945-6954.

3. X. Lu, M.C. Arduini-schuster, J. Kuhn, O. Nilsson, J. Fricke, R.W. Pekala, Thermal Conductivity of Monolithic Organic Aerogels, *Science*, 1992, 255, 971-972.

4. A. Du, H. Wang, B. Zhou, C. Zhang, X. Wu, Y. Ge, T. Niu, X. Ji, T. Zhang, Z. Zhang, G. Wu, J. Shen, Multifunctional Silica Nanotube Aerogels Inspired by Polar Bear Hair for Light Management and Thermal Insulation, *Chem. Mater.*, 2018, 30, 6849–6857.

5. J. Wan, J. Zhang, J. Yu, J. Zhang, Cellulose Aerogel Membranes with a Tunable Nanoporous Network as a Matrix of Gel Polymer Electrolytes for Safer Lithium-Ion Batteries, *ACS Appl. Mater. Interfaces*, 2017, **9**, 24591-24599.